

Electrostatic analysis of the interactions between charged particles of dielectric materials

Elena Bichoutskaia,^{1,a)} Adrian L. Boatwright,¹ Armik Khachatourian,² and Anthony J. Stace¹

¹*School of Chemistry, University of Nottingham, University Park, Nottingham NG7 2RD, United Kingdom*

²*Department of Physics and Astronomy, California State University, Los Angeles, California 90032-4226, USA*

(Received 16 March 2010; accepted 3 June 2010; published online 13 July 2010)

An understanding of the electrostatic interactions that exist between charged particles of dielectric materials has applications that span much of chemistry, physics, biology, and engineering. Areas of interest include cloud formation, ink-jet printing, and the stability of emulsions. A general solution to the problem of calculating electrostatic interactions between charged dielectric particles is presented. The solution converges very rapidly for low values of the dielectric constant and is stable up to the point where particles touch. Through applications to unspecified particles with a range of size and charge ratios, the model shows that there exist distinct regions of dielectric space where particles with the same sign of charge are strongly attracted to one another. © 2010 American Institute of Physics. [doi:10.1063/1.3457157]

I. INTRODUCTION

An understanding of the electrostatic interactions that exist between charged particles of dielectric materials has applications that cover many areas of chemistry, physics, biology, and engineering. Areas of interest include circumstances where charged particles might coalesce, for example, aerosol and water droplets in clouds,¹ dust particles in space,² toner particles in electrophotographic printers,³ and suspensions of charged colloidal spheres.⁴ Other applications exist in situations where interactions between dielectric particles influence charge separation, and an example of this is electrospray ionization.^{5,6} The benefits to be gained from finding a general and convergent solution to the problem of interacting dielectric particles are very significant. Modeling the induced image charge interaction between two conducting spheres that carry a charge has been the subject of many numerical and analytical studies over a number of decades.⁷ In contrast, comparable theoretical studies of interacting dielectric spheres began only quite recently. To date a variety of solutions have been offered, many of which present mathematical derivations with limited applicability, numerical complications, or poor convergence at very short particle separation. Finding a stable solution with universal relevance to the electrostatic properties of two closely interacting dielectric spheres each carrying an arbitrary amount of charge remains a challenge.

An image solution to the problem of a point charge outside a conducting sphere at zero potential was first proposed in 1845 by Thomson (later Lord Kelvin) who interpreted the Legendre series expressing the potential due to the *actual* charge on the sphere as the potential due to an *imaginary* point charge.⁸ Since then the classical Kelvin image theory

for a charged sphere was successfully generalized by Lindell^{9,10} and extended to dielectric spheres.^{11–14} Many models based on the image charge theory exist today, and these include a variety of boundary conditions suitable for describing some aspects of experiment,^{15–17} most notably the methods proposed by Ohshima^{18–24} for the interaction between spheres in media of homogeneous dielectric permittivity. However, at close separation image charge methods require increasing numbers of images leading to convergence problems for a series expansion of the electrostatic force. Alternative approaches to studying electrostatic interactions between dissimilar spherical dielectric particles include bispherical coordinate methods,²⁵ as well as various numerical calculations, for example, Monte Carlo methods²⁶ or the Galerkin finite-element method,³ but these techniques have limited applicability. A variational method to determine surface polarization of dielectrics of arbitrary shape has recently been set forward, and applied to a special case of two dielectric spheres of the same radius and charge.²⁷

A new approach to calculating the electrostatic force acting on a dielectric sphere in an arbitrary external electric field was proposed by Washizu^{28,29} and developed further in a subsequent series of papers.^{30–32} The technique is based on a re-expansion as a Taylor series of a Legendre expansion for the external field around the center of a dielectric sphere. A remarkable feature of the method is that the boundary conditions, which define the problem, can be readily incorporated into a solution by expanding the potential as a Legendre polynomial series.^{33–36} This method has recently been extended to a variety of electrostatic boundary value problems with dielectrics and conductors of spherical geometry.^{37–41} However, for touching spheres a rapid convergence to a stable solution, while maintaining general applicability, has not been achieved.

In this work, a general solution to the problem of two interacting spherical particles of arbitrary size, electrical

^{a)}Author to whom correspondence should be addressed. Electronic mail: elena.bichoutskaia@nottingham.ac.uk.

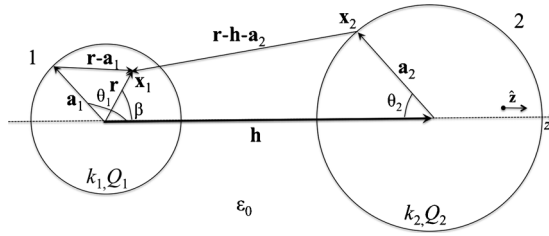


FIG. 1. A general geometric representation of the problem of two interacting dissimilar spheres. Dielectric constants, permanent charges, and the radii of spheres 1 and 2 are denoted as k_1, Q_1, \mathbf{a}_1 and k_2, Q_2, \mathbf{a}_2 , respectively.

charge, and dielectric constant is presented, covering a full range of separation distances including the point of contact. The action of charges under their mutual influence is obtained from Gauss's law that couples uniquely the surface potential with the distribution and magnitude of electrical charge on the surface of the spheres. The effect of the surface charge is integrated to obtain an analytical expression for the electrostatic force acting on the spheres at arbitrary separations. The result is a simple series expression for the force that converges rapidly, can be efficiently generalized to many-body systems for studying interactions in concentrated solutions, and can be readily implemented within a variety of particle collision and coalescence models. The boundary conditions selected for the problem imply a *constant charge system* in which the total net surface charge on each sphere does not change with a variation in distance between spheres. In this solution, no discontinuities in the electric field (or force per unit charge) within the spherical surface are encountered. Through applications to unspecified particles with a range of size and charge ratios, the model shows that there exist distinct regions of dielectric space where particles with the same sign of charge are strongly attracted to one another. These attractions arise from anisotropies in the induced multipole interactions.

II. METHODOLOGY

A. Distribution of the electric potential on the surface of the spheres

As shown in Fig. 1, the considered problem involves two dielectric spheres, denoted as sphere i ($i=1,2$), of an arbitrary size defined by a radius a_i , permittivity ϵ_i , and carrying an arbitrary charge Q_i in a surrounding dielectric medium of permittivity ϵ_0 (free space in this instance). The permittivity of a sphere relative to that of free space is the dimensionless dielectric constant $k_i=\epsilon_i/\epsilon_0$, where the permittivity of free space (vacuum) ϵ_0 is equal to $8.854\,187\,817\,6 \times 10^{-12}$ F/m. The dielectric material is electrically neutral in its normal state with an undisturbed charge distribution, and contains an equal number of positive and negative bound charges, $\sigma_{b,i}$. The charge on each sphere is assumed to be distributed uniformly over the surface, and no volume charge is present. Hence, the total surface charge density σ_i is related to the free and bound charge densities as $\sigma_i=\sigma_{f,i}+\sigma_{b,i}$. The net charge on each sphere is fixed, independent of the dielectric constant, and does not vary with the separation distance between the spheres defined by vector \mathbf{h} . This con-

dition implies a constant free surface charge density, $\sigma_{f,i}$, and the variation in electrostatic force acting on the system is the result of polarization of the bound charge residing on the surface of one sphere induced by an electric field due to the presence of charge on the second sphere.

The Gauss electric potential⁴² at a point \mathbf{r} due to spheres 1 and 2 is given by

$$\Phi(\mathbf{r}) = K \int \frac{dQ}{R} = K \int \frac{\sigma_1(t)dt}{|\mathbf{r} - \mathbf{a}_1(t)|} + K \int \frac{\sigma_2(t)dt}{|\mathbf{r} - \mathbf{h} - \mathbf{a}_2(t)|}, \quad (1)$$

where $K=1/4\pi\epsilon_0 \approx 9 \times 10^9$ Vm/C is a constant of proportionality and the integration is performed over the surfaces of the spheres. The potential $\Phi(\mathbf{r})$ is the sum of the contributions from spheres 1 and 2, and it vanishes at infinity. Equation (1) can be viewed as the time-independent, singular propagator solution of the Poisson two-particle differential equation $\nabla^2\Phi=-4\pi K\sigma$, where ∇^2 is the Laplacian and σ is the charge density which, in this special case, resides only on the surface of the sphere.

In the following two subsections, it is shown how potential (1) can be expanded about the center of each sphere and how boundary conditions are applied to achieve a solution. These steps are taken to treat both spheres.

1. Expansion of the potential in terms of Legendre polynomials

The denominator of the second term in Eq. (1) has no singularity at $\mathbf{r}=\mathbf{a}_1$, hence it can be expanded by a single convergent polynomial about the center of sphere 1 as

$$\begin{aligned} & K \int \frac{\sigma_2(t)dt}{|\mathbf{r} - \mathbf{h} - \mathbf{a}_2(t)|} \\ &= K \int \frac{\sigma_2(\theta_2)a_2^2 \sin \theta_2 d\phi_2 d\theta_2}{|\mathbf{r}(\beta, \phi_\beta) - \mathbf{h} - \mathbf{a}_2(\theta_2, \phi_2)|} \\ &= K \int (2\pi)\sigma_2(\theta_2)a_2^2 \sin \theta_2 d\theta_2 \\ &\quad \times \sum_{l=0}^{\infty} \sum_{m=0}^{\infty} \frac{(l+m)!}{m!l!} \frac{r^l a_2^m}{h^{l+m+1}} P_l(\cos \beta) P_m(\cos \theta_2), \quad (2) \end{aligned}$$

assuming spherical polar coordinates (a_1, θ_1, ϕ_1) , (a_2, θ_2, ϕ_2) , and (r, β, ϕ_β) for vectors \mathbf{a}_1 , \mathbf{a}_2 , and \mathbf{r} , respectively (see Fig. 1). After introducing

$$A_{i,m} = 2\pi K a_i^{m+2} \int_0^\pi \sin \theta_i d\theta_i \sigma_i(\theta_i) P_m(\cos \theta_i), \quad (3)$$

Eq. (2) can be rewritten as

$$K \int \frac{\sigma_2(t)dt}{|\mathbf{r} - \mathbf{h} - \mathbf{a}_2(t)|} = \sum_{l=0}^{\infty} \sum_{m=0}^{\infty} A_{2,m} \frac{(l+m)!}{m!l!} \frac{r^l}{h^{l+m+1}} P_l(\cos \beta). \quad (4)$$

Expansion (4) is valid at all points $r < a_1$ and $r > a_1$ as long as they are outside the region occupied by sphere 2.

The denominator of the first term in Eq. (1) is, however, singular on the surface of sphere 1 where vectors \mathbf{r} and \mathbf{a}_1

coincide, and $|\mathbf{r}-\mathbf{a}_1| \equiv 0$, and so expansion about the center of sphere 1 leads to the separate expressions for $r < a_1$ and $r > a_1$, namely,

$$\begin{aligned} K \int \frac{\sigma_1(t) dt}{|\mathbf{r}-\mathbf{a}_1(t)|} &= K \int \frac{\sigma_1(\theta_1) a_1^2 \sin \theta_1 d\phi_1 d\theta_1}{|\mathbf{r}(\beta, \phi_\beta) - \mathbf{a}_1(\theta_2, \phi_2)|} \\ &= K \int (2\pi) \sigma_1(\theta_1) a_1^2 \sin \theta_1 d\theta_1 \\ &\quad \times \sum_{l=0}^{\infty} \frac{r^l}{a_1^{l+1}} P_l(\cos \beta) P_l(\cos \theta_1) \\ &= \sum_{l=0}^{\infty} A_{1,l} \frac{r^l}{a_1^{2l+1}} P_l(\cos \beta) \quad \text{for } r < a_1 \quad (5) \end{aligned}$$

and

$$\begin{aligned} K \int \frac{\sigma_1(t) dt}{|\mathbf{r}-\mathbf{a}_1(t)|} &= K \int \frac{\sigma_1(\theta_1) a_1^2 \sin \theta_1 d\phi_1 d\theta_1}{|\mathbf{r}(\beta, \phi_\beta) - \mathbf{a}_1(\theta_1, \phi_1)|} \\ &= K \int (2\pi) \sigma_1(\theta_2) a_1^2 \sin \theta_1 d\phi_1 d\theta_1 \\ &\quad \times \sum_{l=0}^{\infty} \frac{a_1^l}{r^{l+1}} P_l(\cos \beta) P_l(\cos \theta_1) \\ &= \sum_{l=0}^{\infty} A_{1,l} \frac{1}{r^{l+1}} P_l(\cos \beta) \quad \text{for } r > a_1. \quad (6) \end{aligned}$$

Substitution of Eqs. (4)–(6) in Eq. (1) gives the expansion of the electric potential in the vicinity of sphere 1 in terms of Legendre polynomials,

$$\begin{aligned} \Phi(\mathbf{r}) &= \sum_{l=0}^{\infty} A_{1,l} \frac{r^l}{a_1^{2l+1}} P_l(\cos \beta) \\ &\quad + \sum_{l=0}^{\infty} \sum_{m=0}^{\infty} A_{2,m} \frac{(l+m)!}{m!l!} \frac{r^l}{h^{l+m+1}} P_l(\cos \beta) \end{aligned}$$

for $r < a_1$,

$$\begin{aligned} \Phi(\mathbf{r}) &= \sum_{l=0}^{\infty} A_{1,l} \frac{1}{r^{l+1}} P_l(\cos \beta) \\ &\quad + \sum_{l=0}^{\infty} \sum_{m=0}^{\infty} A_{2,m} \frac{(l+m)!}{m!l!} \frac{r^l}{h^{l+m+1}} P_l(\cos \beta) \end{aligned}$$

for $r > a_1$. (7)

2. Application of the boundary conditions

Apart from the condition that the electric potential vanishes at infinity, three additional boundary conditions are applied. The first boundary condition is continuity of the potential on the surface of the sphere due to the continuity of the tangential component of the electric field,

$$-\frac{1}{r} \frac{\partial \Phi}{\partial \beta} \Big|_{r=a_1^-} = -\frac{1}{r} \frac{\partial \Phi}{\partial \beta} \Big|_{r=a_1^+}. \quad (8)$$

This boundary condition is automatically satisfied by the choice of the electric potential described by Eq. (1). Note that the potential on the surface of the spheres is not constant. The second boundary condition is discontinuity of the normal component of the electric field due to the presence of a permanent charge on the surface of each sphere,

$$4\pi K \sigma_1 = \frac{\partial \Phi}{\partial r} \Big|_{r=a_1^-} - \frac{\partial \Phi}{\partial r} \Big|_{r=a_1^+}. \quad (9)$$

The last boundary condition states that the normal component of the dielectric displacement field due to the presence of free charge on the surface of a sphere is discontinuous,

$$4\pi K \sigma_{f,1} = k_1 \frac{\partial \Phi}{\partial r} \Big|_{r=a_1^-} - \frac{\partial \Phi}{\partial r} \Big|_{r=a_1^+} = \text{const.} \quad (10)$$

Expansion (7) can be used to express the boundary condition (9) with Legendre polynomials as basis functions

$$4\pi K \sigma_1 = \sum_{l=0}^{\infty} A_{1,l} \frac{la_1^{l-1}}{a_1^{2l+1}} P_l(\cos \beta) + \sum_{l=0}^{\infty} A_{1,l} \frac{l+1}{a_1^{l+1}} P_l(\cos \beta) \quad (11)$$

to give the following expression for the total surface charge density on sphere 1:

$$\sigma_1(\beta) = \frac{1}{4\pi K} \sum_{l=0}^{\infty} A_{1,l} \frac{2l+1}{a_1^{l+2}} P_l(\cos \beta). \quad (12)$$

Similarly, boundary condition (10) gives

$$\begin{aligned} 4\pi K \sigma_{f,1} &= \sum_{l=0}^{\infty} A_{1,l} \frac{k_1 la_1^{l-1}}{a_1^{2l+1}} P_l(\cos \beta) + \sum_{l=0}^{\infty} A_{1,l} \frac{l+1}{a_1^{l+2}} P_l(\cos \beta) \\ &\quad + (k_1 - 1) \sum_{l=0}^{\infty} \sum_{m=0}^{\infty} A_{2,m} \frac{(l+m)!}{m!l!} \frac{la_1^{l-1}}{h^{l+m+1}} P_l(\cos \beta). \end{aligned} \quad (13)$$

Multiplying both sides of Eq. (13) by $\sin \beta P_l(\cos \beta)$ and integrating over the surface of sphere 1 as $\int_0^\pi \sin \beta d\beta P_l(\cos \beta) P_l(\cos \beta) = [2/(2l+1)] \delta_{l,l'}$ gives the following expression for the multipole moments:

$$4\pi K a_1 \sigma_{f,1} \delta_{l,0} = \frac{A_{1,l}}{a_1^{l+1}} + \frac{(k_1 - 1)l}{(k_1 + 1)l + 1} \sum_{m=0}^{\infty} A_{2,m} \frac{(l+m)!}{l!m!} \frac{a_1^l}{h^{l+m+1}}. \quad (14)$$

An expansion of potential (1) about the center of sphere 2 and the subsequent application of boundary conditions, as described above for the case of sphere 1, leads to a complementary equation for multipole moments [this must follow from Eq. (14) by simultaneously interchanging subscripts 1 and 2],

$$4\pi K a_2 \sigma_{f,2} \delta_{l,0} = \frac{A_{2,l}}{a_2^{l+1}} + \frac{(k_2 - 1)l}{(k_2 + 1)l + 1} \sum_{m=0}^{\infty} A_{1,m} \frac{(l+m)!}{l!m!} \frac{a_2^l}{h^{l+m+1}}. \quad (15)$$

After eliminating $A_{2,l}$, Eqs. (14) and (15) can be combined to obtain A_{1,j_1} ,

$$A_{1,j_1} = a_1 V_1 \delta_{j_1,0} - \frac{(k_1 - 1)j_1}{(k_1 + 1)j_1 + 1} \frac{a_1^{2j_1+1}}{h^{j_1+1}} a_2 V_2 + \frac{(k_1 - 1)j_1}{(k_1 + 1)j_1 + 1} \\ \times \sum_{j_2=0}^{\infty} \sum_{j_3=0}^{\infty} \frac{(k_2 - 1)j_2}{(k_2 + 1)j_2 + 1} \frac{(j_1 + j_2)! (j_2 + j_3)!}{j_1! j_2! j_3!} \\ \times \frac{a_1^{2j_1+1} a_2^{2j_2+1}}{h^{j_1+2j_2+j_3+2}} A_{1,j_3}, \quad (16)$$

where $a_1 V_1 = 4\pi K a_1^2 \sigma_{f,1} = K Q_1$; $a_2 V_2 = 4\pi K a_2^2 \sigma_{f,2} = K Q_2$. With an increase in the values of the dielectric constants k_1 and k_2 , an insulator begins to resemble a conductor, and for infinitely large values of k_1 and k_2 , Eq. (16) describes a conductor. It can be seen from Eqs. (14) and (15) that under the ‘‘constant free surface charge’’ boundary condition, if l is set to zero the coefficients $A_{1,0}$ for sphere 1 and $A_{2,0}$ for sphere 2 do not change as a function of the separation distance h .

B. Electrostatic force

To calculate the electrostatic force due to the presence of a permanent charge residing on the surface of each of the two spheres, Coulomb’s law for point charges can be readily generalized. The electrostatic force is given by

$$\mathbf{F}_{12} = K \int dQ_1(\mathbf{x}_1) \int dQ_2(\mathbf{x}_2) \frac{\mathbf{x}_1 - \mathbf{x}_2}{|\mathbf{x}_1 - \mathbf{x}_2|^3} \\ = -\hat{\mathbf{z}} \frac{\partial}{\partial h} \left(K \int dQ_1(\mathbf{x}_1) \int dQ_2(\mathbf{x}_2) \frac{1}{|\mathbf{x}_1 - \mathbf{x}_2|} \right) \Big|_{\sigma_i = \text{const}}, \quad (17)$$

where \mathbf{x}_1 and \mathbf{x}_2 are points on spheres 1 and 2, and $\hat{\mathbf{z}}$ is a unit vector along the z -axis as shown in Fig. 1. The first integral takes into account all charges residing on sphere 1 and the second integral is the potential generated by all charges residing on sphere 2. The last equality in Eq. (17) arises due to cylindrical symmetry of the problem provided the differentiation with respect to the separation distance h is performed keeping the total surface charge density σ_i constant. It is evaluated before applying the boundary condition, as shown below. The convention of a negative term for an attractive contribution to the force and a positive term describing repulsion has been used.

If the vector \mathbf{a}_1 defines point \mathbf{x}_1 on sphere 1 and the vector \mathbf{r} defines point \mathbf{x}_2 on sphere 2, then the distance between two points located on spheres 1 and 2 is

$$|\mathbf{r} - \mathbf{a}_1| = \sqrt{r^2 + a_1^2 - 2a_1 r [\cos \beta \cos \theta_1 + \sin \beta \sin \theta_1 \cos(\phi_\beta - \phi_1)]} \quad (18)$$

and the electrical charge on each sphere is

$$dQ_i = a_i^2 \sin \theta_i d\theta_i d\phi_i \sigma_i(\theta_i). \quad (19)$$

The total charge on each sphere can be found by integrating over all angles as

$$Q_{i,\text{tot}} = 2\pi a_i^2 \int_0^\pi d\theta_i \sigma_i(\theta_i) \sin \theta_i, \quad (20)$$

where $\sigma_i(\theta_i)$ is the total charge density as a function of azimuth angle θ_i .

Using Eqs. (18)–(20) Coulomb force (17) can be rewritten in spherical coordinates as follows:

$$F_{12} = -\frac{\partial}{\partial h} K (a_1 a_2)^2 \int_0^\pi \sin \theta_1 d\theta_1 \sigma_1(\theta_1) \int_0^\pi \sin \theta_2 d\theta_2 \sigma_2(\theta_2) \int_0^{2\pi} d\phi_2 \\ \times \int_0^{2\pi} \frac{d\phi_1}{\sqrt{r^2 + a_1^2 - 2a_1 r [\cos \beta \cos \theta_1 + \sin \beta \sin \theta_1 \cos(\phi_\beta - \phi_1)]}}. \quad (21)$$

To simplify Eq. (21) we note that the integral over ϕ_1 is independent of ϕ_β , and hence it can be written as

$$\int_0^{2\pi} d\phi_2 \int_0^{2\pi} \frac{d\phi_1}{\sqrt{r^2 + a_1^2 - 2a_1 r [\cos \beta \cos \theta_1 + \sin \beta \sin \theta_1 \cos(\phi_\beta - \phi_1)]}} \\ = (2\pi)^2 \sum_{l=0}^{\infty} \frac{a_1^l}{r^{l+1}} P_l(\cos \beta) P_l(\cos \theta_1) = (2\pi)^2 \sum_{l=0}^{\infty} \sum_{m=0}^{\infty} \frac{(l+m)!}{l!m!} \frac{a_1^l a_2^m}{h^{l+m+1}} P_m(\cos \theta_2) P_l(\cos \theta_1), \quad (22)$$

where in the last equality the following identity has been used:

$$\frac{P_l(\cos \beta)}{r^{l+1}} = \sum_{m=0}^{\infty} \frac{(l+m)!}{l!m!} \frac{a_2^m}{h^{l+m+1}} P_m(\cos \theta_2). \quad (23)$$

Substitution of Eq. (22) back into Eq. (21) gives

$$\begin{aligned} F_{12} &= -\frac{\partial}{\partial h} K(2\pi)^2 (a_1 a_2)^2 \sum_{l=0}^{\infty} \sum_{m=0}^{\infty} \frac{(l+m)!}{l!m!} \frac{a_1^l a_2^m}{h^{l+m+1}} \int_0^{\pi} \sin \theta_2 d\theta_2 \sigma_2(\theta_2) P_m(\cos \theta_2) \int_0^{\pi} \sin \theta_1 d\theta_1 \sigma_1(\theta_1) P_l(\cos \theta_1) \\ &= (a_1 a_2)^2 \sum_{l=0}^{\infty} \sum_{m=0}^{\infty} \frac{(l+m+1)!}{l!m!} \frac{a_1^l a_2^m}{h^{l+m+2}} \int_0^{\pi} \sin \theta_2 d\theta_2 \sigma_2(\theta_2) P_m(\cos \theta_2) \int_0^{\pi} \sin \theta_1 d\theta_1 \sigma_1(\theta_1) P_l(\cos \theta_1). \end{aligned} \quad (24)$$

Using Eq. (3), Eq. (24) can be simplified as follows:

$$F_{12} = \frac{1}{K} \sum_{l=0}^{\infty} \sum_{m=0}^{\infty} A_{1,l} A_{2,m} \frac{(l+m+1)!}{l!m!} \frac{1}{h^{l+m+2}} \quad (25)$$

and after rearrangement using Eq. (14) the electrostatic force is given by

$$\begin{aligned} F_{12} &= \frac{1}{K} \sum_{l=0}^{\infty} A_{1,l} (l+1) \sum_{m=0}^{\infty} A_{2,m} \frac{(l+m+1)!}{(l+1)!m!} \frac{1}{h^{l+m+2}} = \frac{1}{K} \sum_{l=0}^{\infty} A_{1,l} \frac{(k_1+1)(l+1)+1}{(k_1-1)a_1^{l+1}} \left(K a_1 \sigma_{f,1} \delta_{l+1,0} - \frac{A_{1,l+1}}{a_1^{l+2}} \right) \\ &= -\frac{1}{K} \sum_{l=0}^{\infty} A_{1,l} A_{1,l+1} \frac{(k_1+1)(l+1)+1}{(k_1-1)a_1^{2l+3}}. \end{aligned} \quad (26)$$

In third line of Eq. (26) the dependence of the electrostatic force between two spheres on the separation distance h is held in the multipole moments coefficients $A_{1,l}$ and $A_{1,l+1}$. The coefficients are computed by solving the linear Eq. (16) and substituted back in the third line of Eq. (26) to investigate the behavior of the electrostatic force numerically. The results are discussed in Sec. IV.

III. PHYSICAL AND MATHEMATICAL CONSIDERATIONS

In Eq. (26), the $l=0$ term can be separated from the summation as follows:

$$\begin{aligned} F_{12} &= \frac{1}{K} \sum_{l=0}^{\infty} A_{1,l} (l+1) \sum_{m=0}^{\infty} A_{2,m} \frac{(l+m+1)!}{(l+1)!m!} \frac{1}{h^{l+m+2}} = \frac{1}{K} \left[A_{1,0} \sum_{m=0}^{\infty} A_{2,m} \frac{m+1}{h^{m+2}} + \sum_{l=1}^{\infty} A_{1,l} (l+1) \sum_{m=0}^{\infty} A_{2,m} \frac{(l+m+1)!}{(l+1)!m!} \frac{1}{h^{l+m+2}} \right] \\ &= \frac{1}{K} \left[A_{1,0} \sum_{m=0}^{\infty} A_{2,m} \frac{m+1}{h^{m+2}} + \sum_{l=1}^{\infty} A_{1,l} \frac{(k_1+1)(l+1)+1}{(k_1-1)a_1^{l+1}} \left(K a_1 \sigma_{f,1} \delta_{l+1,0} - \frac{A_{1,l+1}}{a_1^{l+2}} \right) \right] \\ &= \frac{1}{K} \left[A_{1,0} \sum_{m=0}^{\infty} A_{2,m} \frac{m+1}{h^{m+2}} - \sum_{l=1}^{\infty} A_{1,l} A_{1,l+1} \frac{(k_1+1)(l+1)+1}{(k_1-1)a_1^{2l+3}} \right]. \end{aligned} \quad (27)$$

Further rearrangement using Eq. (15) gives

$$F_{12} = \frac{1}{K} \left[\frac{A_{1,0} A_{2,0}}{h^2} + A_{1,0} \sum_{m=1}^{\infty} \sum_{l=0}^{\infty} A_{1,l} \frac{(k_2-1)m}{(k_2+1)m+1} \frac{(l+m+1)!}{l!m!} \frac{a_2^{2m+1}}{h^{2m+l+2}} \right] - \frac{1}{K} \sum_{l=1}^{\infty} A_{1,l} A_{1,l+1} \frac{(k_1+1)(l+1)+1}{(k_1-1)a_1^{2l+3}}. \quad (28)$$

Taking into account the equalities $A_{1,0}=KQ_1=4\pi Ka_1^2\sigma_{1,f}$ and $A_{2,0}=KQ_2=4\pi Ka_2^2\sigma_{2,f}$, the electrostatic force can be written as

$$F_{12} = K \frac{Q_1 Q_2}{h^2} - Q_1 \sum_{m=1}^{\infty} \sum_{l=0}^{\infty} A_{1,l} \frac{(k_2 - 1)m(m+1)}{(k_2 + 1)m + 1} \times \frac{(l+m)! a_2^{2m+1}}{l!m! h^{2m+l+3}} - \frac{1}{K} \sum_{l=1}^{\infty} A_{1,l} A_{1,l+1} \frac{(k_1 + 1)l + 1}{(k_1 - 1)a_1^{2l+3}}. \quad (29)$$

The first term in Eq. (29) is the Coulomb force between two nonpolarizable spheres, or point charges separated by a distance h ,

$$F_{12}^0 = K \frac{Q_1 Q_2}{h^2}, \quad (30)$$

the first and second terms taking $l=0$ as the electrostatic force between a charged polarizable sphere 2 and a nonpolarizable sphere 1 (or a point charge),

$$F_{12}^1 = K \frac{Q_1 Q_2}{h^2} - K \frac{Q_1^2}{h^2} \sum_{m=1}^{\infty} \frac{(k_2 - 1)m(m+1) a_2^{2m+1}}{(k_2 + 1)m + 1 h^{2m+1}}. \quad (31)$$

Thus, we obtain a solution for the electrostatic force between two dissimilar dielectric, charged, polarizable spheres, where specific case (31) for $Q_2=0$ is well known from the theory of static and dynamic electricities as the attraction between a neutral polarizable sphere and a point charge.⁴³ If sphere 2 is nonpolarizable ($k_2=1$), the electrostatic force is simply defined by the first term of Eq. (31), and for the case $Q_1 Q_2 > 0$ the force is always repulsive irrespective of how large the charge, Q_2 , is on sphere 2. When sphere 2 is polarizable ($k_2 > 1$) the second term in Eq. (31) becomes attractive, but the first term will be either attractive or repulsive depending on the signs of the charges Q_1 and Q_2 . In the case of a dielectric sphere, under the action of an external force (in this case, due to the presence of a nonpolarizable sphere with charge Q_1), the bound charges experience a torque and the dipoles and higher order multipoles align within sphere 2 along the electric field generated by the nonpolarizable sphere. If Q_1 is negative the Coulomb field aligns the positive bound charges to face sphere 1 giving rise to the net attractive force, and if Q_1 is positive the negative bound charges are aligned which also give a net attractive force. The larger the dielectric constant the greater the effective alignment and hence the greater the attractive force; however, the probability of a bound charge becoming free would also increase, and this would cause the dielectric material to resemble a conductor. Similar effects occur throughout the volume of the sphere but since there is no free volume charge density it follows that there cannot be a bound volume charge density. Hence the absence of a volume term in the equation of force (17). In the next section, we discuss in detail the effects of surface polarization in dielectric spheres on the net electrostatic force.

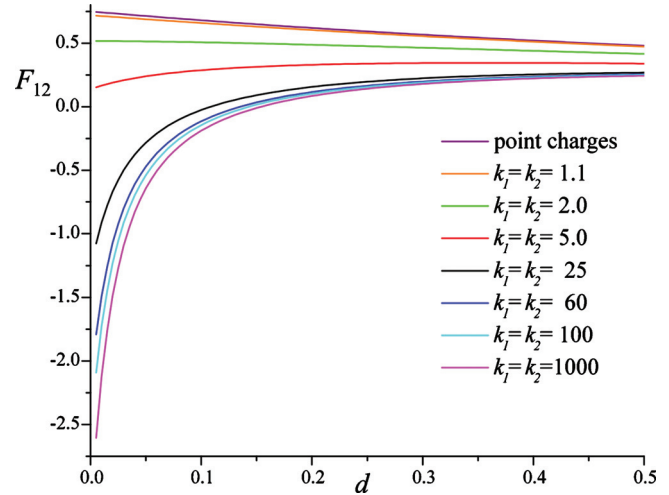


FIG. 2. Calculated electrostatic force, F_{12} , between two spheres as a function of the scaled separation d . In each case, $a_1=a_2$, $Q_1=1$, and $Q_2=3$, and the value of dielectric constant, k_i , varies between 1.1 and 1000. For reference purposes, the force between two point charges has also been plotted.

IV. DISCUSSION AND RESULTS

In this first application of the model the calculations concentrate on one of the more interesting aspects to the behavior of charged particles, and that is when particles carrying the same sign of charge are attracted to one another. In clouds this process is called charge scavenging and takes the form of highly charged aerosols being absorbed by much larger, charged water droplets.^{44,45} Laboratory experiments have confirmed this behavior and current models of charge scavenging use image charge methods.^{1,44,45} More recently, there has been interest in the electrostatic interactions that exist between like-charged colloidal particles when they are suspended in an electrolyte.⁴ Again, experiments support the view that under certain circumstances, these interactions can be attractive. In situations where particle dispersion is important, for example, in the case of electrospray, the attractive electrostatic interactions between highly charged fragments as they begin to move apart can generate a barrier to separation. To date, image charge methods have been used to model this behavior.⁵

In this section the conditions under which an attraction between like-charge particles of a dielectric material might be observed are mapped out for various combinations of size, charge, and dielectric constant. In all cases, the particles are assumed to be suspended in a vacuum, and so no account has been taken of how the presence of a solvent might moderate the strength of an interaction. In the discussion that follows the variables of distance and charge are presented as dimensionless ratios, which means that the observed patterns of behavior are appropriate for particles with absolute sizes and charges that can vary over many orders of magnitude. Distance d presented in Figs. 2–4 is a scaled separation between the surfaces of two spheres defined as $d=(h-(a_1+a_2))/a_1$. Similarly, the calculated electrostatic force between the particles, F_{12} , has been scaled. Figure 2 shows how F_{12} varies as a function of scaled separation d between two spheres of equal radius, $a_2/a_1=1$, where $Q_2/Q_1=3$, and for a wide range of dielectric constants. For

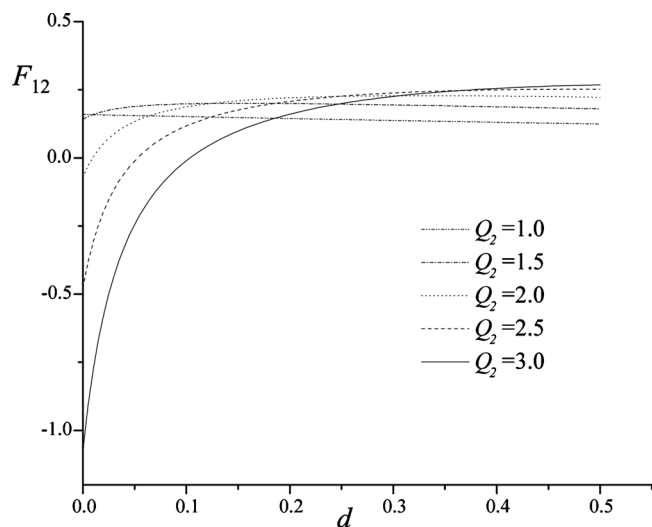


FIG. 3. Calculated electrostatic force, F_{12} , between two spheres as a function of the scaled separation d . In each case, $a_1=a_2$, $k_i=25$, and the charge ratio, Q_2/Q_1 , varies between 1 and 3.

reference purposes, the force between two point charges is also given. As can be seen, when the dielectric constant is small F_{12} remains positive and tends to the limit of nonpolarizable spheres or point charges described by solution (30). However, as k_i increases beyond 5 the force becomes increasingly more negative at short separations, and this is indicative of an attractive interaction between the particles. What is clear is that the most significant changes in F_{12} take place when the dielectric constant varies between 2 and 25 where, for a given value of d the forces switch from being repulsive, $F_{12} > 0$, to attractive, $F_{12} < 0$, at short separations. As k_i approaches 1000 the spheres start to behave as conductors and the very strong attraction characteristic of charged metallic particles with different radii is observed.⁷ Figure 3 takes the data for $k_i=25$ and shows how F_{12} varies as a function of the charge ratio Q_2/Q_1 . In this case it can be seen that as the latter increases there is a very significant increase in the degree of attraction between the spheres. However,

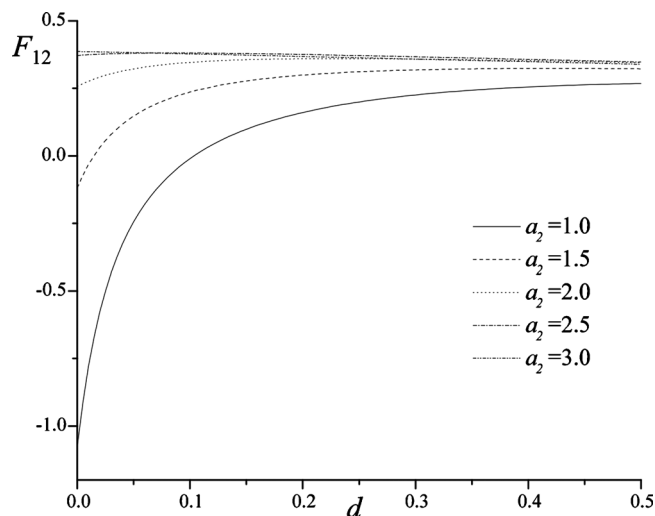


FIG. 4. Calculated electrostatic force, F_{12} , between two spheres as a function of the scaled separation d . In each case, $Q_2/Q_1=3$, $k_i=25$, and the ratio of the radii, a_2/a_1 , varies between 1 and 3.

this attraction is counterbalanced, in part, by a repulsive interaction at long range that also increases as a function of Q_2/Q_1 . Finally for this section, Fig. 4 shows how the electrostatic force between spheres with $k_i=25$ and $Q_2/Q_1=3$ varies as a function of d for different ratios of their size. As can be seen, the strongest attraction exists when sphere 2 is small and has the higher surface charge density. As the latter decreases (sphere 2 increases in size), the force rapidly switches to being greater than zero, which corresponds to a repulsive interaction.

Having established that attractive interactions between particles are at their strongest when the two spheres touch, Fig. 5 presents a series of three-dimensional plots of the force between two touching particles calculated as a function of systematic changes in the two ratios Q_2/Q_1 and a_2/a_1 for a range of dielectric constants. In Fig. 5(a) both spheres have a dielectric constant of 1.1 and it is clear that irrespective of charge or size, the force is always positive and so the interaction is repulsive. As noted earlier, this situation corresponds to spheres that are nonpolarizable. In contrast, when $k_i=100$ [Fig. 5(b)] there is a very marked region of attraction when Q_2/Q_1 is greater than unity and a_2/a_1 is less than unity; however, there is also an area of the plot corresponding to Q_2/Q_1 less than unity and a_2/a_1 greater than unity that is also weakly attractive (see below). In Figs. 5(c) and 5(d), the model has been applied to two spheres carrying opposite charges and, as expected, the interaction is always attractive, but its magnitude is strongly influenced by dielectric constant. Finally, in Figs. 5(e) and 5(f) an analysis of the interaction between spheres with different dielectric constants is presented. Again, the magnitude of the force is affected by the value assigned to either of the dielectric constants and is at its strongest (most negative) when the particle with the larger charge is given a low value of k_i . As expected, this result implies that a large sphere with a high value of k_i is very susceptible to being polarized by a highly charged body. In Fig. 5(e) it is again possible to identify a combination of $Q_2/Q_1 < 1$ and $a_2/a_1 > 1$ where the force becomes negative and the circumstances are similar to those responsible for the strong attraction in Fig. 5(f): a large polarizable sphere in the presence of a smaller sphere that is carrying a higher charge.

From the patterns of behavior displayed in Fig. 5 it is clear that the switch between like-charged particles experiencing either a positive or a negative force (a repulsive or attractive interaction) is critically dependent on the values assigned to Q_2/Q_1 , a_2/a_1 , k_1 , and k_2 . From an analysis of how surfaces, such as those give in Fig. 5, respond to systematic changes in these variables, it is possible to map out those regions of Q_2/Q_1 , a_2/a_1 , k_1 , and k_2 where the force is either positive under any circumstances or becomes negative at close separation. For each value of $k_1=k_2 < 1000$ the ratios of Q_2/Q_1 and a_2/a_1 at which the force switches from being positive to negative have been determined and plotted in Fig. 6. For clarity, the number of discrete values for k_i presented on the plot has been limited, but sufficient results are shown to define boundaries. Taking, for example, $a_2/a_1=2$, it can be seen that when $k_i=1000$ there will be an attractive interaction between particles when Q_2/Q_1 is either less than 1 or greater than 3. Similarly, when $k_i=5$, the same size ratio will need a

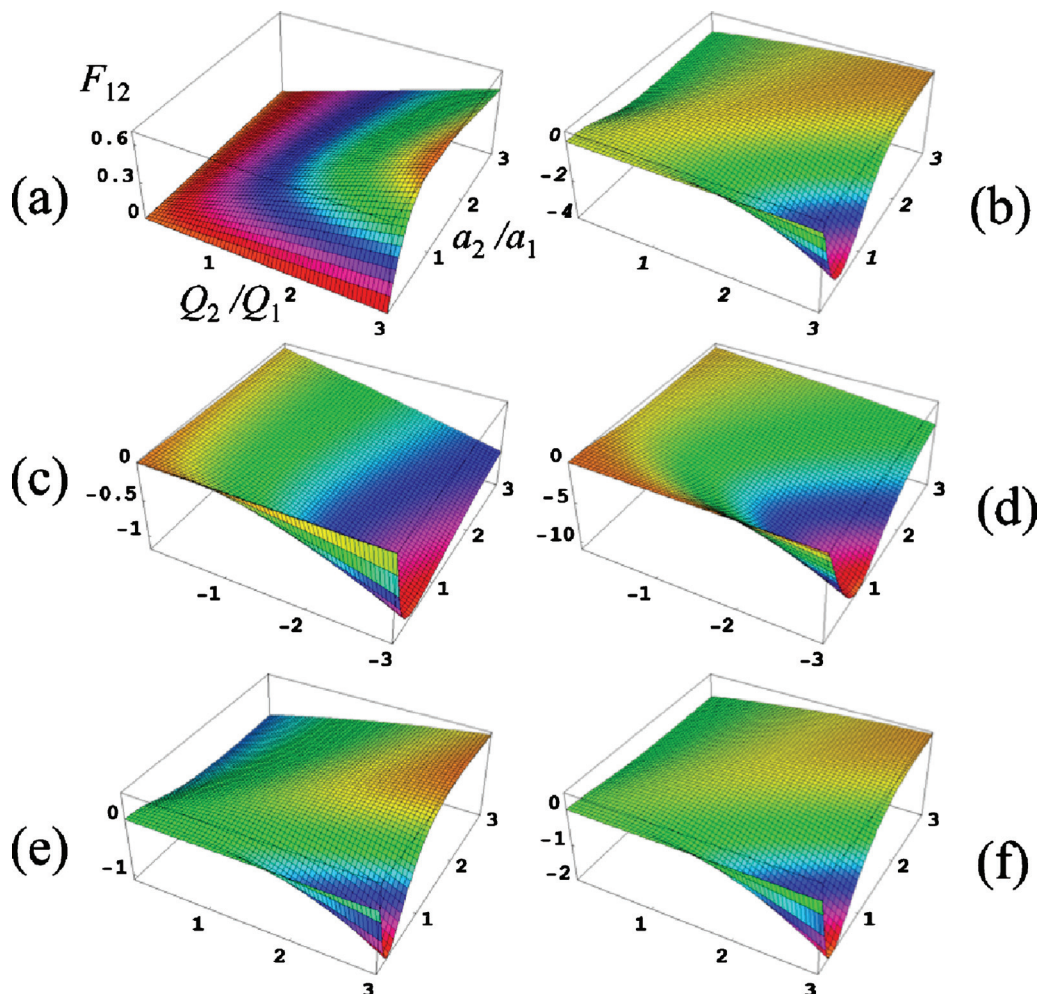


FIG. 5. Three-dimensional plots showing the variation of the electrostatic force, F_{12} , between touching spheres ($d=0$) as the charge ratio, Q_2/Q_1 , and the ratio of the radii, a_2/a_1 , vary between 0 and 3. (a) $k_1=k_2=1.1$; (b) $k_1=k_2=100$; (c) and (d), as for (a) and (b), but one of the sphere carries a negative charge; (e) $k_1=5$, $k_2=100$; (f) $k_1=100$, $k_2=5$. Note the second attractive region in (e) when Q_2/Q_1 is much less than 1 and a_2/a_1 is in the range of 2–3. The color is only a guide and does not denote any absolute scale.

charge ratio on the particles, Q_2/Q_1 , which is either very small or greater than 7 for the pair to experience an attractive interaction. Going in the other direction, it is clear that the constraints on creating an attractive combination are far more restrictive. For example, if $Q_2/Q_1=1$, then a_2/a_1 has to be either less than 1 or greater than 2 ($k_i > 25$), alternatively if $k_i=5$ then a_2/a_1 has to be either very much smaller than 1 or greater than 6. No particles of that charge ratio will experience an attraction if $k_i < 5$. Beyond $Q_2/Q_1=2$, the model predicts that the interaction between like-charged particles will always be repulsive when $a_2/a_1 > 4$. As expected, these regions also map onto the surfaces shown in Fig. 5. Taking for example Fig. 5(b), then the two attractive sections identified above correspond in Fig. 6 to situation where Q_2/Q_1 is either much less than 1 (weakly attracting) or greater than 3 (strongly attracting).

V. CONCLUSIVE REMARKS

A general solution to the problem of calculating the electrostatic interaction between two charged particles of a dielectric material has been presented. The solution converges very rapidly for low values of the dielectric constant and it is

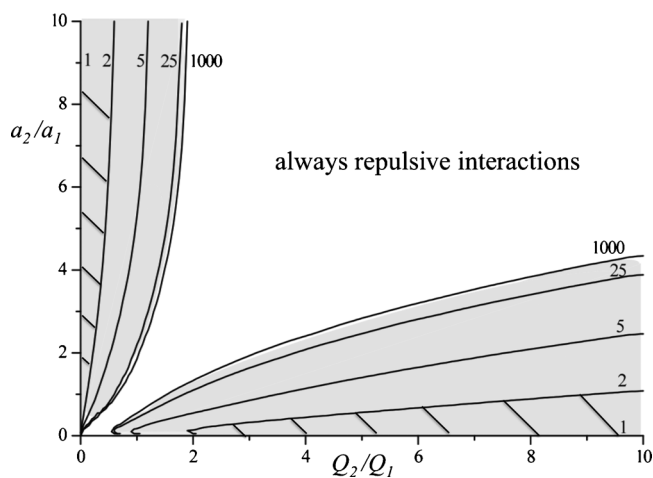


FIG. 6. A map showing the regions of Q_2/Q_1 and a_2/a_1 where the electrostatic force, F_{12} , between touching particles becomes negative, and particles are attracted to one another. Contours have been calculated for selected values of $k_1=k_2$ in the range of 1–1000, and are presented as boundaries, within which particles carrying the same sign of charge are attracted to one another. For example, the regions of attractive interactions for $k_1=k_2=1000$ are shown by gray shaded areas and for $k_1=k_2=2$ by dashed areas; for $Q_2/Q_1=4$ the conditions for attraction are $a_2/a_1 < 1$ if $k_1=k_2=5$ and $a_2/a_1 < 2$ if $k_1=k_2=25$.

stable up to the point where the particles touch. The excellent convergence of the solution for the electrostatic force has been achieved through elimination of angular dependence from the final equations. It is shown that with the application of certain limiting conditions, the solution for the force fully agrees with an earlier result from the application of classical electrostatics to the problem of a point charge interacting with a neutral polarizable sphere. By mapping out how the force between arbitrary charged particles varies according to their dielectric constant, it is shown that there are very distinct ratios of charge (Q_2/Q_1) and size (a_2/a_1) that lead to an attractive interaction between particles of like-charged.

ACKNOWLEDGMENTS

E.B. gratefully acknowledges financial support from an EPSRC-GB Career Acceleration Fellowship (EP/G005060/1). Authors would like to acknowledge Dr. R. J. Wheatley for his critical reading of the manuscript and Nottingham University for financial support.

$$U_{12} = K(a_1 a_2)^2 \int_0^\pi \sin \theta_1 d\theta_1 \sigma_1(\theta_1) \int_0^\pi \sin \theta_2 d\theta_2 \sigma_2(\theta_2) \int_0^{2\pi} d\phi_2 \int_0^{2\pi} \frac{d\phi_1}{\sqrt{r^2 + a_1^2 - 2a_1 r [\cos \beta \cos \theta_1 + \sin \beta \sin \theta_1 \cos(\phi_\beta - \phi_1)]}}. \quad (\text{A2})$$

Substitution of identity (23) into Eq. (A2) gives

$$U_{12} = K(2\pi)^2 (a_1 a_2)^2 \sum_{l=0}^{\infty} \sum_{m=0}^{\infty} \frac{(l+m)!}{l!m!} \frac{a_1^l a_2^m}{h^{l+m+1}} \int_0^\pi \sin \theta_2 d\theta_2 \sigma_2(\theta_2) P_m(\cos \theta_2) \int_0^\pi \sin \theta_1 d\theta_1 \sigma_1(\theta_1) P_l(\cos \theta_1). \quad (\text{A3})$$

Using Eq. (3), Eq. (A3) can be simplified as follows:

$$\begin{aligned} U_{12} &= \frac{1}{K} \sum_{l=0}^{\infty} \sum_{m=0}^{\infty} \frac{(l+m)!}{l!m!} \frac{1}{h^{l+m+1}} A_{1,l} A_{2,m} \\ &= \frac{1}{K} \sum_{m=0}^{\infty} \frac{1}{h^{m+1}} A_{1,0} A_{2,m} + \frac{1}{K} \sum_{l=1}^{\infty} \sum_{m=0}^{\infty} \frac{(l+m)!}{l!m!} \\ &\quad \times \frac{1}{h^{l+m+1}} A_{1,l} A_{2,m}, \end{aligned} \quad (\text{A4})$$

and further rearrangement using Eq. (14) as $A_{1,0} = KQ_1 = 4\pi K a_1^2 \sigma_{1,f}$ gives

$$\begin{aligned} U_{12} &= Q_1 \frac{A_{2,0}}{h} + Q_1 \sum_{m=1}^{\infty} \frac{A_{2,m}}{h^{m+1}} + \frac{1}{K} \sum_{l=1}^{\infty} A_{1,l} \frac{1}{a_1^l} \frac{(k_1+1)l+1}{(k_1-1)l} \\ &\quad \times \left(4\pi K a_1 \sigma_{f,1} \delta_{l,0} - \frac{A_{1,l}}{a_1^{l+1}} \right). \end{aligned} \quad (\text{A5})$$

Taking into account the equality $A_{2,0} = KQ_2 = 4\pi K a_2^2 \sigma_{2,f}$, further rearrangement gives

APPENDIX A: COULOMB ENERGY BETWEEN TWO CHARGED PARTICLES OF A DIELECTRIC MATERIAL

Although application of the theory of electrostatics to the interpretation of experimental data on dielectric particles frequently requires a measure of the force, F_{12} , there are many instances where knowledge of the potential energy between colliding particles is required. In this appendix the equations presented earlier have been reformulated to give an expression for the Coulomb energy between two charged particles of a dielectric material.

The Coulomb interaction energy is given by

$$U_{12} = K \int dQ_1(\mathbf{x}_1) \int \frac{dQ_2(\mathbf{x}_2)}{|\mathbf{x}_1 - \mathbf{x}_2|}, \quad (\text{A1})$$

where \mathbf{x}_1 and \mathbf{x}_2 are points on spheres 1 and 2 as shown in Fig. 1. Using Eqs. (18)–(20) the Coulomb interaction potential (A1) can be rewritten in spherical coordinates as follows:

$$\begin{aligned} U_{12} &= K \frac{Q_1 Q_2}{h} + Q_1 \sum_{m=1}^{\infty} \frac{A_{2,m}}{h^{m+1}} - \frac{1}{K} \sum_{l=1}^{\infty} \frac{(k_1+1)l+1}{(k_1-1)l} \frac{A_{1,l} A_{1,l}}{a_1^{2l+1}} \\ &= K \frac{Q_1 Q_2}{h} + Q_2 \sum_{m=1}^{\infty} \frac{A_{1,m}}{h^{m+1}} - \frac{1}{K} \sum_{l=1}^{\infty} \frac{(k_2+1)l+1}{(k_2-1)l} \frac{A_{2,l} A_{2,l}}{a_2^{2l+1}}. \end{aligned} \quad (\text{A6})$$

Finally, using Eqs. (14) and (15) we can rewrite the first line of Eq. (A6) as

$$\begin{aligned} U_{12} &= K \frac{Q_1 Q_2}{h} - Q_1 \sum_{m=1}^{\infty} \sum_{l=0}^{\infty} \frac{(k_2-1)m}{(k_2+1)m+1} \frac{(l+m)!}{l!m!} \\ &\quad \times \frac{a_2^{2m+1}}{h^{2m+l+2}} A_{1,l} - \frac{1}{K} \sum_{l=1}^{\infty} \frac{(k_1+1)l+1}{(k_1-1)l} \frac{A_{1,l} A_{1,l}}{a_1^{2l+1}} \end{aligned} \quad (\text{A7})$$

and the second line of Eq. (A6) can be also rewritten by interchanging labels 1 and 2.

APPENDIX B: CONVERGENCE RATES

The convergence rates of summations for the electrostatic force and the Coulomb energy are, in general, much slower for conductors than for dielectric materials. To dem-

TABLE I. Convergence test for Eq. (26) calculating the electrostatic force between two identical charged dielectric particles at the point of contact. The force is presented as $F_{12}=(V^2/K)S$, where S is the result of the summation in Eq. (26) and $V=V_1=V_2$ (particles have the same charge Q and the same radius a). Column 1 shows the number of terms (n) in the summation of Eq. (26). Changes in the value of S are shown in columns 2 and 3 for a small value of the dielectric constant ($k=2$) and a very large value ($k=1000$).

n	S	
	$k=2$	$k=1000$
15	0.210 013 309 5	0.153 867 218
20	0.210 013 298 8	0.153 866 796
25	0.210 013 297 5	0.153 866 795
30	0.210 013 297 4	0.153 866 795

onstrate the excellent convergence rate of the presented formalism, the most demanding computationally case of two spheres in contact is presented in Table I, in which the two spheres are assumed identical ($Q_1=Q_2$ and $a_1=a_2$). As Table I shows with the limit taken to be 30 precision of ten decimal places (absolute error is 3×10^{-9}) is achieved for large values of the dielectric constant ($k=1000$) and more than ten decimal places (absolute error is 8×10^{-11}) for small values of the dielectric constant ($k=2$).

¹H. T. Ochs III and R. R. Czys, *Nature (London)* **327**, 606 (1987).

²A. A. Sickafoose, J. E. Colwell, M. Horányi, and S. Robertson, *Phys. Rev. Lett.* **84**, 6034 (2000).

³J. Q. Feng, *Phys. Rev. E* **62**, 2891 (2000).

⁴E. Allahyarov, E. Zaccarelli, F. Sciortino, P. Tartaglia, and H. Löwen, *Europhys. Lett.* **78**, 38002 (2007).

⁵M. Labowsky, J. B. Fenn, and J. Fernandez de la Mora, *Anal. Chim. Acta* **406**, 105 (2000).

⁶P. Kebarle and M. Peschke, *Anal. Chim. Acta* **406**, 11 (2000).

⁷U. Näher, S. Bjornholm, S. Frauendorf, F. Garcias, and C. Guet, *Phys. Rep.* **285**, 245 (1997).

⁸W. Thomson (Lord Kelvin), *J. Math. Pures Appl.* **10**, 364 (1845); **12**, 256 (1847); *Papers on Electrostatics and Magnetism*, 2nd ed. (Macmillan, London, 1884), Pts. 75–127, p. 208 (reprint).

⁹J. C.-E. Sten and I. V. Lindell, *J. Electromagn. Waves Appl.* **9**, 599 (1995).

¹⁰I. V. Lindell, G. Dassios, and K. I. Nikoskinen, *J. Phys. D: Appl. Phys.* **34**, 2302 (2001).

¹¹I. V. Lindell, J. C.-E. Sten, and K. I. Nikoskinen, *Radio Sci.* **28**, 319 (1993).

¹²I. V. Lindell and K. I. Nikoskinen, *J. Electromagn. Waves Appl.* **15**, 1075 (2001).

¹³D. V. Redžić and S. S. Redžić, *J. Electromagn. Waves Appl.* **17**, 1625 (2003).

¹⁴D. V. Redžić, *J. Phys. D: Appl. Phys.* **38**, 3991 (2005).

¹⁵J. L. Marin and R. Rosas, *Am. J. Phys.* **52**, 358 (1984).

¹⁶J. A. Soules, *Am. J. Phys.* **58**, 1195 (1990).

¹⁷J. Sliško and R. A. Brito-Orta, *Am. J. Phys.* **66**, 352 (1998).

¹⁸H. Ohshima and T. Kondo, *J. Colloid Interface Sci.* **155**, 499 (1993).

¹⁹H. Ohshima and T. Kondo, *Colloid Polym. Sci.* **271**, 1191 (1993).

²⁰H. Ohshima, *J. Colloid Interface Sci.* **162**, 487 (1994).

²¹H. Ohshima, *J. Colloid Interface Sci.* **170**, 432 (1995).

²²H. Ohshima, *J. Colloid Interface Sci.* **176**, 7 (1995).

²³H. Ohshima, E. Mishonova, and E. Alexov, *Biophys. Chem.* **57**, 189 (1996).

²⁴H. Ohshima, *J. Colloid Interface Sci.* **328**, 3 (2008).

²⁵M. H. Davis, *Am. J. Phys.* **37**, 26 (1969).

²⁶M.-S. Chun and W. R. Bowen, *J. Colloid Interface Sci.* **272**, 330 (2004).

²⁷R. Allen and J.-P. Hansen, *J. Phys.: Condens. Matter* **14**, 11981 (2002).

²⁸M. Washizu, *J. Electrostat.* **29**, 177 (1993).

²⁹M. Washizu and T. B. Jones, *J. Electrostat.* **33**, 187 (1994).

³⁰T. Matsuyama, H. Yamamoto and M. Washizu, *J. Electrostat.* **36**, 195 (1995).

³¹M. Washizu and T. B. Jones, *IEEE Trans. Ind. Appl.* **32**, 233 (1996).

³²Y. Nakajima and T. Sato, *J. Electrostat.* **45**, 213 (1999).

³³A. V. M. Khachatourian and A. O. Wistrom, *J. Phys. A* **36**, 6495 (2003).

³⁴A. V. M. Khachatourian and A. O. Wistrom, *J. Colloid Interface Sci.* **242**, 52 (2001).

³⁵A. V. M. Khachatourian and A. O. Wistrom, *J. Phys. A* **33**, 307 (2000).

³⁶A. O. Wistrom and A. V. M. Khachatourian, *Meas. Sci. Technol.* **10**, 1296 (1999).

³⁷T. P. Doerr and Y.-K. Yu, *Am. J. Phys.* **72**, 190 (2004).

³⁸T. P. Doerr and Y.-K. Yu, *Phys. Rev. E* **73**, 061902 (2006).

³⁹Y.-K. Yu, *Physica A* **326**, 522 (2003).

⁴⁰P. Linse, *J. Chem. Phys.* **128**, 214505 (2008).

⁴¹B. J. Cox, N. Thamwattana and J. M. Hill, *J. Electrostat.* **65**, 680 (2007).

⁴²C. F. Gauss, *Resultate aus den beobachtungen des magnetischen verins im jahre 1839* (Leipzig, 1840) [*Scientific Memoirs, Selected from the Transactions of Foreign Academies of Science and Learned Societies N 7* (Johnson, New York, 1840), p.153 (English translation)].

⁴³W. R. Smythe, *Static and Dynamic Electricity*, 2nd ed. (McGraw-Hill, New York, 1950).

⁴⁴B. A. Tinsley, *Rep. Prog. Phys.* **71**, 066801 (2008).

⁴⁵S. N. Tripathi and R. G. Harrison, *Atmos. Res.* **62**, 57 (2002).